

Iron oxidation and order–disorder in the (Fe²⁺, Mn)(Ta, Nb)₂O₆ → (Fe²⁺, Mn)Fe³⁺(Ta, Nb)₂O₈ transition

C A dos Santos[†], L I Zawislak, V Antonietti, E J Kinast and J B M da Cunha
Instituto de Física, UFRGS, CP 15051, Campus do Vale, 91501-970 Porto Alegre, RS, Brazil
E-mail: cas@if.ufrgs.br

Received 5 January 1999, in final form 5 July 1999

Abstract. Heat treatments in air and in vacuum have been performed on crystal and powder of the natural tantalite (Mn_{0.88}²⁺Fe_{0.09}²⁺)(Ta_{0.86}⁵⁺Nb_{0.14}⁵⁺)₂O₆²⁻, as well as on powder of synthetic Fe²⁺(Nb_{0.6}⁵⁺Ta_{0.4}⁵⁺)₂O₆. Crystal parameters and hyperfine interactions were obtained by use of x-ray diffraction and Mössbauer spectroscopy. It is shown that the partially ordered natural sample is completely ordered after heat treatment in vacuum. Conversely, heat treatment in air induced the tantalite [(Mn_{0.88}²⁺Fe_{0.09}²⁺)(Ta_{0.86}⁵⁺Nb_{0.14}⁵⁺)₂O₆²⁻] → wodginite [(Mn²⁺, Fe²⁺)Fe³⁺(Ta, Nb)₂O₈] transformation on the powdered sample. When applied to the crystal sample, the heat treatment in air produced a mixture of two phases: the one in large amount is the ordered (Mn_{0.88}²⁺Fe_{0.09}²⁺)(Ta_{0.86}⁵⁺Nb_{0.14}⁵⁺)₂O₆²⁻, the other, in minor amount, is (Mn_{0.88}²⁺Fe_{0.09}²⁺)Fe³⁺(Ta, Nb)₂O₈. The former arrives from cation ordering in the bulk portion of the sample, while the latter results from the near-surface oxidation. The Mn content as well as the oxidant atmosphere appears to play an important role in the transition mechanism. The same heat treatment applied to the synthetic columbite induces a different reaction: ferrocolumbite is transformed into the ixiolite Fe³⁺(Nb_{0.6}Ta_{0.4})O₄ with a minor amount of (Nb, Ta)₂O₅.

1. Introduction

The mineral columbite—tantalite (sometimes referred to simply as columbite, for Nb > Ta, or tantalite, for Ta > Nb) is a solid solution of the AB₂O₆ type. It includes ferrocolumbite (FeNb₂O₆), manganocolumbite (MnNb₂O₆), manganotantalite (MnTa₂O₆) and ferrotantalite (FeTa₂O₆) as end members and crystallizes in the orthorhombic space group *Pbcn* with an ordered α -PbO₂ superstructure [1, 2]. Closely related to this system are the minerals wodginite [3] and ixiolite [4]. The former, with the general formula ABC₂O₈ (A = Mn, Fe²⁺; B = Sn, Ti, Fe³⁺, Ta; C = Ta, Nb), crystallize in the monoclinic space group *C2/c* [5, 6], while ixiolite, with general formula MO₂ (M = Mn, Sn, Fe, Ta, Nb), is a columbite substructure [4].

Idealized sections of these structures, projected along the *a*-axis, are outlined in figure 1. The A and B octahedra in figure 1 refer to the wodginite structure. For columbite both octahedra correspond to the A site, occupied by Fe and Mn cations, while the C sites for wodginite correspond to the B sites for columbite, occupied by Ta and Nb cations. In the context of the present investigation, an ordered columbite means all Fe and Mn occupying the A site, while all Ta and Nb occupy the B site. It does not mean order between Mn and Fe on A sites.

[†] Corresponding author.

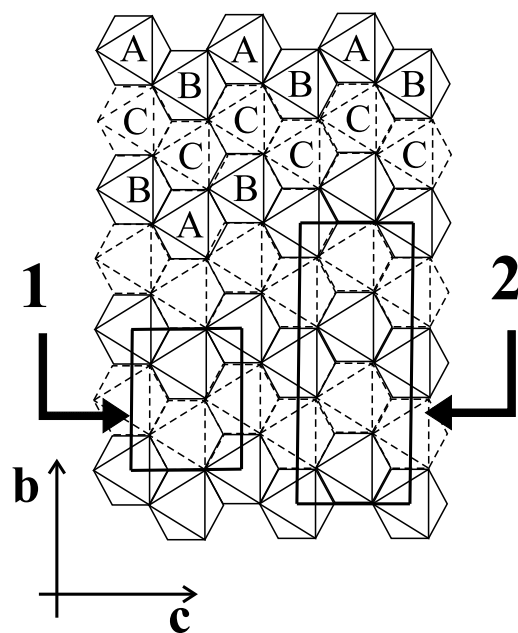


Figure 1. Idealized section of the α - PbO_2 structure projected along the a -axis. A, B and C refer to the cations on the general formula, ABC_2O_8 , for wodginite. Occupied octahedra in the upper level are shown in full lines; those occupied in the next level down are shown in broken lines. The columbite and ixiolite cells are represented by the rectangle (1), while rectangle (2) represents the wodginite cell. The ixiolite cell is one double layer deep, wodginite is two double layers deep, and columbite is three double layers deep.

In the idealized wodginite structure, ABC_2O_8 , one layer of C cations follows each layer of A + B cations. In the idealized columbite structure, AB_2O_6 , layers of A cations at $x = 0$ and $1/2$ are separated by two layers of B cations at $x = 1/6$ and $2/6$. Previous structure investigations [2, 5] have shown that columbite and wodginite can be considered as different superstructures of the α - PbO_2 -like structure of ixiolite.

Order–disorder phenomena relating these minerals have been extensively investigated [5–11]. Cation ordering in the MO_2 structure is possible if the size of the unit cell is increased [6]. To satisfy symmetry restrictions on this process, two alternatives are possible. In the first one the MO_2 cell is tripled, given the AB_2O_6 structure. In the other alternative the cell is quadrupled, given the ABC_2O_8 structure. Therefore, fully disordered AB_2O_6 compounds and fully disordered ABC_2O_8 compounds can be misidentified as MO_2 compounds. This fact has produced considerable experimental mistakes and misconceptions, as reported during the last three decades. For instance, heating experiments have been used to distinguish these materials, with the generally accepted assumption that heating of the mineral ixiolite reveals a wodginite x-ray powder diffraction (XRPD) pattern, whereas heating of the disordered columbite (incorrectly called pseudo-ixiolite) yields an ordered columbite pattern characterized by its superstructure reflections [4]. However, calculation of a theoretical powder diffraction pattern of fully ordered manganocolumbite, MnNb_2O_6 , yields only low intensities for the superstructure reflections, namely $I_{200}/I_{311} = 0.096$ and $I_{110}/I_{311} = 0.030$ [10]. Thus, it is difficult to distinguish between MO_2 and partially ordered AB_2O_6 by means of their XRPD pattern, even when done by complex and time-consuming procedures based on Rietveld refinement [10].

If from the structural point of view it is sure that order–disorder transition can transform MO_2 into AB_2O_6 or into ABC_2O_8 , there is, to our knowledge, no clear explanation for the role played by the several variables on each one of these processes. It is not known, for instance, if the alternative transformations are governed by geochemical, or simply by crystallochemical factors. Certainly more crystal chemistry studies are needed for a complete picture.

As heating experiments are, by far, the main source of data on this subject, some relevant results will be briefly reviewed here. Turnock [12] showed that when synthesized in air, $MnFeTa_2O_8$ can be formed in a small composition range, just while there is sufficient Mn to fill the A site, but does not form in the absence of Fe^{3+} . That is to say, some of the Fe atoms should pertain to the B site, while the Mn atoms and the rest of the Fe atoms can share the A site. This result has led to the conjecture that $MnFeTa_2O_8$, instead of $(Mn, Fe)Ta_2O_6$, will form when the system $FeTa_2O_6$ – $MnTa_2O_6$ is heated in an oxidizing atmosphere. Shortly after, Gouder de Beauregard *et al* [13] demonstrated that, upon heating in air, $(Mn, Fe)Ta_2O_6$ shows an XRPD pattern quite similar to that of $MnFeTa_2O_8$. They also observed that the x-ray patterns of $(Mn, Fe)Ta_2O_6$ are unaffected when the samples are heated in an inert atmosphere. Graham and Thornber [2] reported that oxidation of $(Mn, Fe)(Nb, Ta)_2O_6$ with a high Fe/Mn ratio produces a second columbite with a smaller unit cell. The fact that $MnFe(Nb, Ta)_2O_8$ did not form in their experiment was attributed to the high Nb content. Although the results from Gouder de Beauregard *et al* [13] are 30 years old, there is, to our knowledge, only the effort of Graham and Thornber [2] to re-examine this subject. Yet recent papers [1, 6, 8, 10, 11, 14] have casually dismissed the $(Mn, Fe)Ta_2O_6 \rightarrow MnFeTa_2O_8$ transformation, although they have discussed the related $(Mn, Fe, Ta)O_2 \rightarrow MnFeTa_2O_8$ transition.

In addition to these inherent complexities, reports on the subject are sometimes dubious. For instance, descriptions of heating experiments are frequently incomplete. Heating in air, in a reducing atmosphere, or in vacuum, will certainly produce different reactions. Also, heating a powdered or a crystal sample in air will produce different oxidation effects, because for the latter one the area available for oxidation is smaller. Therefore, these kinds of experimental condition need to be known. Recently it was stated that heating coarse crystal fragments in air at 1000 °C for 16 h induces cation order in $(Mn, Fe)Ta_2O_6$ and results in no significant oxidation of bulk Fe^{2+} , as monitored by unit-cell parameters [11].

The aim of the present paper is to investigate the thermal behaviour and cation ordering on a partially ordered natural Mn-rich tantalite and on an ordered synthetic ferrocolumbite. This is done by use of Mössbauer spectroscopy (MS), as this method is a very efficient tool to investigate the oxidation state of iron, as well as its site occupation. The starting materials and end product were also characterized by x-ray powder diffraction (XRPD).

2. Sample description

The natural sample was a prismatic crystal collected from the Boqueirão pegmatite, in the Rio Grande do Norte State, Northeast of Brazil [15]. From electron probe microanalysis [9] the sample composition has been calculated to be approximately $(Mn_{0.88}^{2+}Fe_{0.09}^{2+})(Ta_{0.86}^{5+}Nb_{0.14}^{5+})_2O_6^{2-}$. In the following this sample is called $(Mn, Fe)Ta_2O_6$. The synthetic ferrocolumbite $Fe(Nb_{0.6}Ta_{0.4})_2O_6$ was prepared by mixing appropriate amounts of powdered Fe, Fe_2O_3 , Ta_2O_5 and Nb_2O_5 . Pellets of the mixture were heated under a nitrogen flow at 1320 K. After 24 h it was cooled at 32 K h⁻¹ and ground. New pellets were again submitted to the same heat treatment for 24 h, followed by the same slow cooling. Hereafter this synthetic sample is called $Fe(Nb, Ta)_2O_6$.

3. Experimental procedures

3.1. Thermal treatments

Thermal treatments of the natural sample were performed on crystal fragments ($\approx 0.5 \text{ cm} \times 0.5 \text{ cm} \times 0.5 \text{ cm}$) and on powdered crystal fragments. Part of the powder was used for the heating experiment in air, while the other part was pelleted and encapsulated in quartz ampoules under vacuum ($P \approx 10^{-5} \text{ Pa}$). In order to compare with published results [2, 4, 13], all the samples were heated at 1320 K for 48 h and subsequently slowly cooled at 32 K h^{-1} . This cooling rate is adequate for cation ordering, e.g., all Fe + Mn in site A and all Ta + Nb in site B of the AB_2O_6 structure [9]. The same heating procedures were used for the synthetic sample.

3.2. X-ray powder diffraction

XRPD patterns were obtained in Bragg–Brentano geometry by means of a Siemens diffractometer D500, equipped with a curved graphite monochromator and Cu $K\alpha$ radiation (Cu $K\alpha_1 = 1.5406 \text{ \AA}$, Cu $K\alpha_2 = 1.5444 \text{ \AA}$) and calibrated with polycrystalline Si. Measurements were performed with a scan step of $0.02^\circ 2\theta$ in the 2θ range from 5° to 100° , with a fixed counting time of 4 s. The program FULLPROF [16] was used for structure refinement.

3.3. Mössbauer spectroscopy

Absorbers for the MS measurements were prepared with appropriate amounts of ground (320 mesh) material in order to satisfy the ideal absorber thickness approximation [17]. The spectra were taken at 80 K and 300 K, using a constant acceleration electromechanical drive system with a multichannel analyser for collecting and storing the data. The velocity scale was calibrated using a high-purity Fe foil. The hyperfine parameters were obtained by a least-squares procedure assuming Lorentzian line shapes constrained to equal halfwidths. ^{57}Co in rhodium was used at room temperature as a source, with nominal activity of 25 mCi. Typical errors are $\pm 3\%$ on hyperfine parameters and $\pm 5\%$ on site occupancies.

4. Results

4.1. X-ray powder diffraction

4.1.1. Powdered natural sample heat treated in vacuum. Representative parts of the XRPD patterns for all the samples are shown in figure 2. A summary of the crystallographic parameters is displayed in table 1. The XRPD pattern for the powdered natural manganotantalite heat-treated in vacuum (PNH vacuum) is quite similar to that for the as-collected sample, but shows a small increase in the relative intensity of the superstructure reflections. That is, $I_{200}/I_{311} = 0.08$ and $I_{110}/I_{311} = 0.03$, while for the as-collected sample $I_{200}/I_{311} = 0.05$ and $I_{110}/I_{311} = 0.02$. Both patterns were indexed to the space group $Pbcn$, with lattice parameters (see table 1) similar to those reported for natural and synthetic tantalite–columbite [1, 4, 5, 7, 10, 11]. Since there are no spurious reflections on the XRPD diagram we conclude that the natural sample is a single-phase Mn-rich tantalite.

4.1.2. Powdered natural sample heated in air. The XRPD pattern for the powdered natural sample heated in air (PNH air) was fitted to three phases. The major one was indexed to the space group $C2/c$, with lattice parameters (see table 1) similar to those reported for wodginite from Rwanda [18]. Additional low intensity reflections can be attributed to monoclinic ixiolite

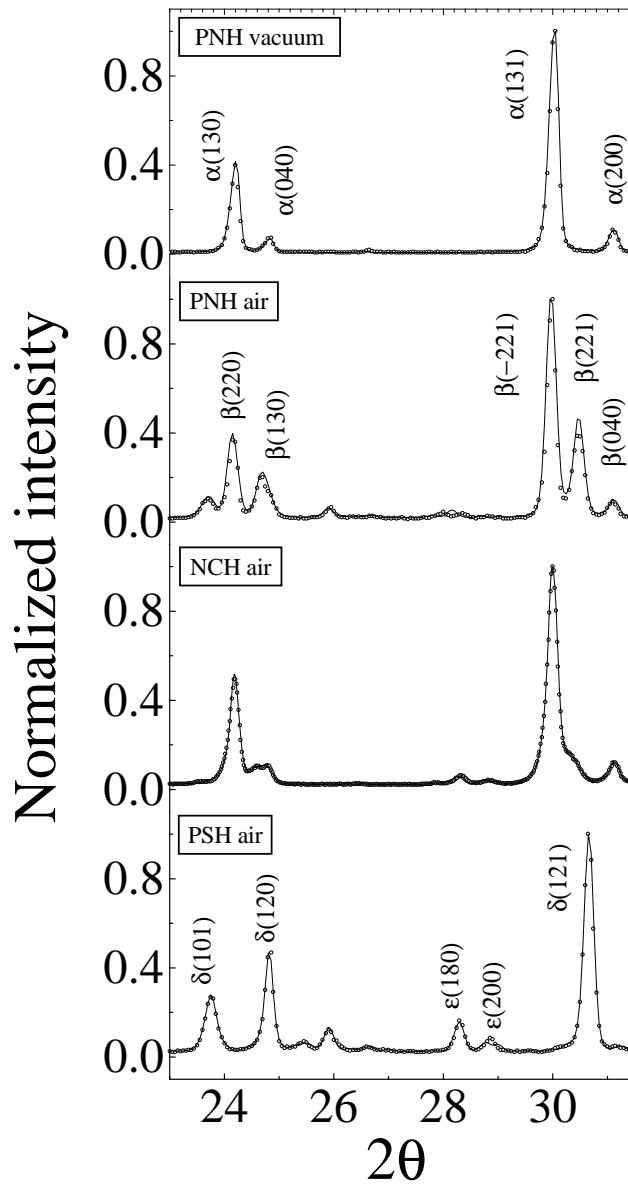


Figure 2. Representative parts of the x-ray powder diffraction patterns for all the samples: powdered natural heated (PNH) in vacuum, powdered natural heated in air, fragments of natural crystal heated (NCH) in air and powdered synthetic heated (PSH) in air. Open circles represent observed data. The solid line represents the calculated pattern obtained with the Rietveld refinement. Tantalite, wadginite, ixiolite and $(Nb, Ta)_2O_5$ reflections are indicated, respectively, by α , β , δ and ϵ .

with space group $P2/c$ and lattice parameters (see table 1) quite close to those reported by Roth and Waring [19], and to monoclinic $(Nb, Ta)_2O_5$ with space group $P2$. The pattern attributed to wadginite ($MnFeTa_2O_8$) is well characterized by the existence of strong peaks at $d \cong 2.95 \text{ \AA}$ ($2\theta \cong 30.29^\circ$) and $d \cong 2.98 \text{ \AA}$ ($2\theta \cong 29.98^\circ$) corresponding to (221) and $(\bar{2}21)$ reflections, respectively.

Table 1. Crystallographic parameters obtained in the present work. PNH vac, PNH air, NCH air, as-prep and PSH air stand for, respectively: powdered natural sample heat treated in vacuum; powdered natural sample heat treated in air; natural crystal heated treated in air; synthetic sample; powdered synthetic sample heat treated in air. *Pbcn*, *C2/c*, *P2/c* and *P2* are space groups for the respective structures: columbite–tantalite; wodginite; ixiolite and monoclinic (Nb, Ta)₂O₅. Numbers in brackets designate $\pm 1\sigma$ on the last decimal given.

Sample	Space group	<i>a</i> (Å)	<i>b</i> (Å)	<i>c</i> (Å)	β (°)	R_B^a
PNH vac	<i>Pbcn</i>	14.3196(9)	5.7413(4)	5.0624(3)	90	5.76
PNH air	<i>C2/c</i>	8.779(4)	12.145(2)	5.089(1)	89.37	4.01
	<i>P2/c</i>	4.682(9)	5.647(28)	5.030(18)	90.14	2.13
	<i>P2</i>	20.429(2)	3.825(1)	19.461(3)	115.49	3.86
NCH air	<i>Pbcn</i>	14.3487(9)	5.7459(5)	5.0779(3)	90	1.22
	<i>C2/c</i>	9.0856(16)	12.0672(9)	5.0470(8)	88.29	2.34
	<i>P2/c</i>	4.7238(9)	5.6205(9)	5.0143(20)	90.81	1.24
	<i>P2</i>	20.4834(8)	3.8230(2)	19.4597(9)	115.38	1.57
As-prep	<i>Pbcn</i>	14.2737(2)	5.7354(1)	5.0554(1)	90	5.55
PSH air	<i>P2/c</i>	4.6493(8)	5.6221(7)	5.0089(7)	90.20	1.76
	<i>P2</i>	20.4022(27)	3.8322(3)	19.4007(16)	115.23	2.57

$$^a R_B = 100 \sum |I_{obs} - I_{calc}| / \sum I_{obs}.$$

4.1.3. Natural crystal heated in air. The heat treatment as described above, applied to natural crystal in air (NCH air) produced a somewhat different result, as viewed by the XRPD pattern (see figure 2). The reflections attributed to MnFeTa₂O₈ are clearly less intense as compared to those observed for PNH air. Note, for instance, the strong decrease of $\beta(130)$ and $\beta(221)$ reflections. Following the refinement procedure it can be seen that the effect of heating a crystal sample is to produce a mixture of four phases; the one in largest amount is the ordered (Mn, Fe)Ta₂O₆ (sg *Pbcn*). Minor reflections were indexed to MnFeTa₂O₈ (sg *C2/c*), (Mn, Fe)(Ta, Nb)O₄ (sg *P2/c*) and (Ta, Nb)₂O₅ (sg *P2*). The former arrives from cation ordering in the bulk portion of the sample, while the minor contributions result from the near-surface oxidation.

4.1.4. Synthetic ferrocolumbite heated in air. The as-prepared Fe(Nb, Ta)₂O₆ sample is single phase, since the XRPD pattern (figure 3) shows no spurious reflections. It was indexed to the space group *Pbcn*, with cell parameters (see table 1) similar to those reported previously for the tantalite–columbite series [1, 4, 5, 7, 10]. The XRPD pattern for the powdered synthetic sample heated in air (PSH air) was indexed to a mixture of two phases. The major one is monoclinic ixiolite, with space group *P2/c* and lattice parameters (see table 1) similar to those reported by Roth and Waring [19]. The one with weak reflections is the monoclinic oxide (Nb, Ta)₂O₅, with space group *P2* and lattice parameters (see table 1) similar to those reported in the JCPDS card No 37-1468. Therefore, supposing mass conservation during the oxidation process and taking into account the XRPD results, the compound Fe(Nb_{0.6}, Ta_{0.4})O₄, hereafter Fe(Nb, Ta)O₄, is the main product resulting from the oxidation of the synthetic ferrocolumbite Fe(Nb_{0.6}Ta_{0.4})₂O₆.

4.2. Mössbauer spectroscopy

4.2.1. As-collected sample. As earlier reported [9], the room-temperature (RT) MS spectrum of the untreated natural sample was fitted to two doublets (see table 2) with ⁵⁷Fe hyperfine parameters characteristic of Fe²⁺ high spin in octahedral coordination. The

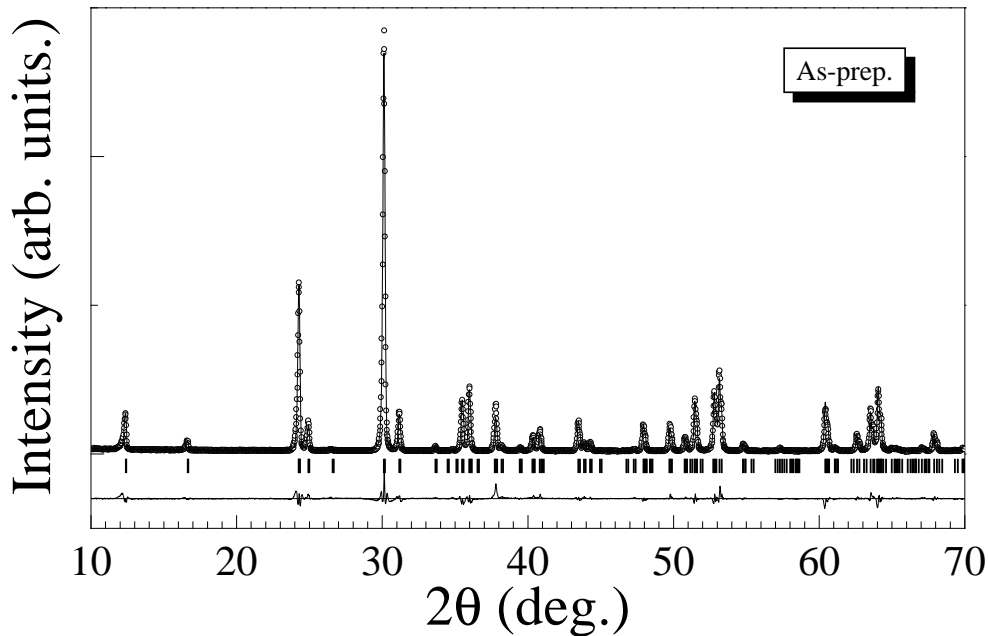


Figure 3. Room-temperature x-ray powder diffraction pattern for the synthetic $Fe(Nb_{0.6}Ta_{0.4})_2O_6$ sample. Open circles represent observed data. The solid line represents the calculated pattern obtained with the Rietveld refinement. The lower trace is a plot of the residual spectrum, observed minus calculated intensities.

spectrum taken at 80 K (in the following, LN spectrum) was fitted to two doublets with $\Delta E_Q = 2.21 \pm 0.07 \text{ mm s}^{-1}$ and $\Delta E_Q = 2.66 \pm 0.08 \text{ mm s}^{-1}$ (see figure 4(a) and table 2). The inner quadrupole splitting increases from 1.55 mm s^{-1} at RT to 2.21 mm s^{-1} at 80 K. Such a thermal behaviour has been observed in ordered $FeNb_2O_6$ [20].

4.2.2. Powdered natural sample heated in vacuum. A previous experiment [9] has shown a dramatic change in the RT spectrum of the natural sample after heat treatment in vacuum. The obtained results are displayed in table 2. In the present study the NL spectrum (figure 4(b) and table 2) was fitted to a doublet with $\Delta E_Q = 2.29 \pm 0.07 \text{ mm s}^{-1}$. This thermal evolution is in complete accord with the above result concerning the temperature dependence of the quadrupole splitting attributed to Fe^{2+} in FeO_6 octahedra in the as-collected sample. This indicates the correctness of the site assignment for the as-collected sample, i.e., the inner doublet is attributed to Fe^{2+} in FeO_6 octahedra, while the outer one is attributed to Fe^{2+} in TaO_6 octahedra.

4.2.3. Powdered natural sample heated in air. The RT spectrum for the natural sample heat treated in air (PNH air) is shown in figure 5(a). It was fitted to two doublets with $\Delta E_Q = 0.52 \pm 0.02 \text{ mm s}^{-1}$ and $\Delta E_Q = 0.34 \pm 0.01 \text{ mm s}^{-1}$ (table 2), attributed to high-spin Fe^{3+} in octahedral coordination. As discussed above, there are two different sites for Fe^{3+} in the wadginite structure: one of them is the B site and the other is the C site. Bearing in mind the great similarity between the outer doublet and that reported ($\Delta E_Q = 0.54 \text{ mm s}^{-1}$, $\delta_{Fe} = 0.39 \text{ mm s}^{-1}$) for a synthetic Fe^{3+} -rich wadginite [14], we have attributed that larger

Table 2. Hyperfine parameters for all measurements reported in the present work. As-coll, PNH vac, PNH air, NCH air, as-prep and PSH air stand for, respectively: untreated natural sample; powdered natural sample heat treated in vacuum; natural sample heat treated in air; crystal fragment of the natural sample heat treated in air; as-prepared synthetic sample and powdered synthetic sample heat-treated in air. ΔE_Q is the quadrupole splitting at the iron sites; δ_{Fe} is the isomer shift relative to α -Fe; $\Gamma \pm 0.01$ is the linewidth at half height; A is the site occupancy, given by the relative spectral area. Uncertainties on the last figures are reported in brackets.

Sample	Temp. (K)	ΔE_Q (mm s ⁻¹)	δ_{Fe} (mm s ⁻¹)	Γ (mm s ⁻¹)	A (%)	Site assignment
As-coll	300	1.55(5)	1.13(3)	0.40	71(4)	FeO ₆
		2.26(7)	1.09(3)	0.47	29(1)	TaO ₆
	80	2.21(7)	1.27(4)	0.44	66(3)	FeO ₆
		2.66(8)	1.25(4)	0.35	34(2)	TaO ₆
PNH vac.	300	1.58(5)	1.14(3)	0.32	100	FeO ₆
	80	2.29(7)	1.27(4)	0.34	100	FeO ₆
PNH air	300	0.52(2)	0.40(1)	0.31	78(4)	FeO ₆
		0.34(1)	0.39(1)	0.33	22(1)	TaO ₆
	80	0.59(2)	0.52(2)	0.30	52(3)	FeO ₆
		0.40(1)	0.49(1)	0.28	48(2)	TaO ₆
NCH air	300	0.55(2)	0.44(1)	0.44	29(1)	FeO ₆
		0.32(1)	0.43(1)	0.41	25(1)	TaO ₆
		1.51(4)	1.13(3)	0.47	41(2)	FeO ₆
	80	2.26(7)	1.14(3)	0.43	5(2)	TaO ₆
		0.61(2)	0.54(2)	0.33	28(1)	FeO ₆
		0.43(1)	0.52(2)	0.30	24(1)	TaO ₆
As-prep	300	2.17(6)	1.26(4)	0.38	26(1)	FeO ₆
		2.59(8)	1.27(4)	0.37	22(1)	TaO ₆
	80	1.78(5)	1.15(3)	0.32	100	FeO ₆
		2.51(8)	1.27(4)	0.32	100	FeO ₆
PSH air	300	0.37(1)	0.40(1)	0.30	100	FeO ₆
	80	0.39(1)	0.51(2)	0.30	100	FeO ₆

quadrupole splitting to Fe³⁺ at FeO₆ octahedra (site B) and the smallest one to Fe³⁺ at TaO₆ octahedra (site C). The smallest quadrupole is also quite similar to that attributed to ixiolite (see section 4.2.6). Therefore, it is reasonable to suppose a mixture of contributions from wodginite site C and ixiolite. These results confirm those obtained with XRD, and clearly show that (Mn, Fe)Ta₂O₆ transforms into wodginite. Following Ferguson *et al* [5], the present wodginite will be designated simply MnFeTa₂O₈. As shown in figure 5(b) and table 2, the LN spectrum for MnFeTa₂O₈ was fitted to two doublets, with $\Delta E_Q = 0.59 \pm 0.02$ mm s⁻¹ and $\Delta E_Q = 0.40 \pm 0.01$ mm s⁻¹.

4.2.4. Natural crystal heated in air. The XRD results have shown that the effect of heating in air a crystal fragment of the (Mn, Fe)Ta₂O₆ sample is to produce a mixture of (Mn, Fe)Ta₂O₆ and MnFeTa₂O₈, with minor reflections indexed to (Fe, Mn)(Ta, Nb)O₄ and (Nb, Ta)₂O₅. Consequently complex Mössbauer spectra are expected for this kind of sample. In fact, as shown in figure 5(c) and figure 5(d), the RT and NL spectra for the natural crystal sample heated in air (NCH air) clearly contain contribution from Fe²⁺ and Fe³⁺ ions. These spectra were fitted to four doublets: $\Delta E_Q = 0.55 \pm 0.02$ mm s⁻¹, $\Delta E_Q = 0.32 \pm 0.01$ mm s⁻¹, $\Delta E_Q = 1.51 \pm 0.04$ mm s⁻¹ and $\Delta E_Q = 2.26 \pm 0.07$ mm s⁻¹ at 300 K and $\Delta E_Q = 0.61 \pm 0.02$ mm s⁻¹, $\Delta E_Q = 0.43 \pm 0.01$ mm s⁻¹, $\Delta E_Q = 2.17 \pm 0.06$ mm s⁻¹ and $\Delta E_Q = 2.59 \pm 0.08$ mm s⁻¹ at 80 K.

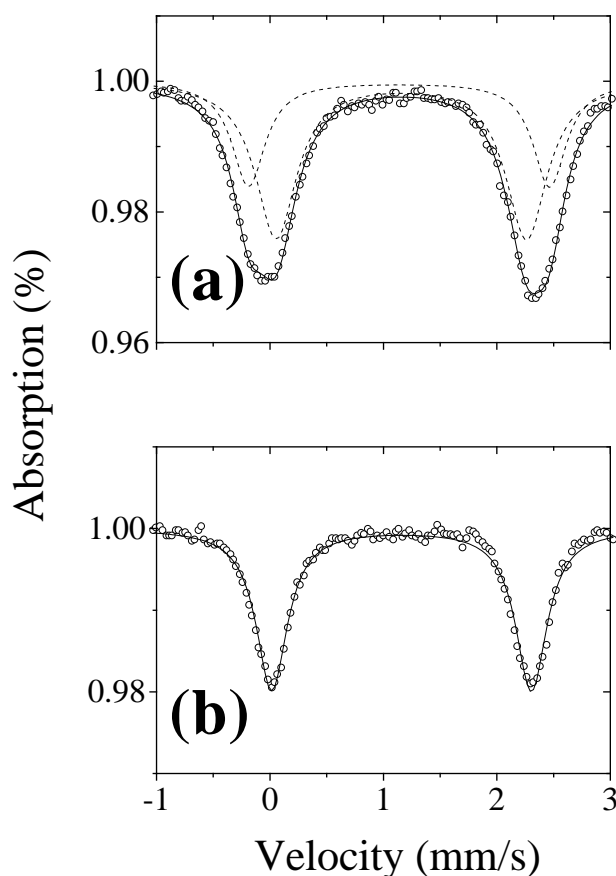


Figure 4. Mössbauer spectra taken at 80 K for: (a) as-collected natural sample; (b) powdered natural sample heat-treated in vacuum. Open circles represent observed data. Solid lines represent the calculated spectra based on a least-squares procedure. Broken lines represent the calculated subspectra.

The site assignment followed that used before for the as-collected and PNH air samples. Thus, at RT $\Delta E_Q = 0.55 \text{ mm s}^{-1}$ and $\Delta E_Q = 1.51 \text{ mm s}^{-1}$ are attributed, respectively, to Fe^{3+} and Fe^{2+} at FeO_6 octahedra, while $\Delta E_Q = 0.32 \text{ mm s}^{-1}$ and $\Delta E_Q = 2.26 \text{ mm s}^{-1}$ are attributed, respectively, to Fe^{3+} and Fe^{2+} at TaO_6 octahedra. The thermal behaviours for all the doublets are similar to those observed for the as-collected sample and for the powder natural sample heated in air as well.

4.2.5. Synthetic ferrocolumbite: as prepared. The RT spectrum for the as-prepared $Fe(Nb_{0.6}Ta_{0.4})_2O_6$ sample is shown in figure 6(a). The existence of only one narrow doublet is indicative of high-degree cation ordering. It was fitted (see table 2) to $\Delta E_Q = 1.78 \pm 0.05 \text{ mm s}^{-1}$ and $\delta_{Fe} = 1.15 \pm 0.03 \text{ mm s}^{-1}$. The LN spectrum, shown in figure 6(b), was fitted to $\Delta E_Q = 2.51 \pm 0.08 \text{ mm s}^{-1}$ and $\delta_{Fe} = 1.27 \pm 0.04 \text{ mm s}^{-1}$. These hyperfine parameters are close to those earlier reported for $FeNb_2O_6$ [20, 21]. The relative increasing of the quadrupole splitting from RT to LN is extraordinary similar to that reported by Eibschütz *et al* [20]. As will be discussed below, the fact that the quadrupole splitting from our sample is larger than that measured for $FeNb_2O_6$ is presumably due to the presence of Ta.

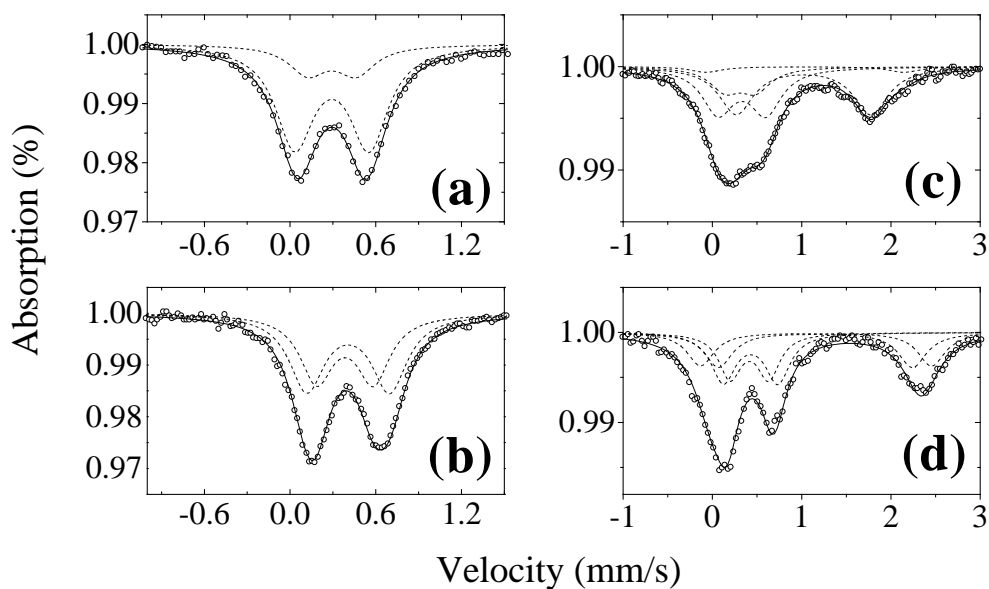


Figure 5. Mössbauer spectra for: (a) powdered natural sample heat treated in air, taken at 300 K; (b) ditto, taken at 80 K; (c) fragments of natural crystal sample heated (NCH) in air, taken at 300 K; (d) ditto, taken at 80 K. Open circles represent observed data. Solid lines represent the calculated spectra based on a least-squares procedure. Broken lines represent the calculated subspectra.

4.2.6. *Synthetic ferrocolumbite: heated in air.* Figure 6(c) displays the RT MS spectrum for the powder synthetic sample heated in air (PSH air), which was identified, from the x-ray measurements, as $\text{Fe}(\text{Nb}, \text{Ta})\text{O}_4$. It was fitted to $\Delta E_Q = 0.37 \pm 0.01 \text{ mm s}^{-1}$ and $\delta_{\text{Fe}} = 0.40 \pm 0.01 \text{ mm s}^{-1}$. Such hyperfine parameters are attributed to Fe^{3+} in octahedral coordination. Consistently with the results obtained for PNH air and NCH air samples, the hyperfine parameters for the PSH air sample at 80 K are quite similar to those measured at RT, as can be seen in figure 6(d) and table 2.

5. Discussion

Firstly, let us recall that all the samples used in the present work are orthorhombic or monoclinic. The as-collected sample, $(\text{Mn}, \text{Fe})(\text{Ta}, \text{Nb})_2\text{O}_6$, is a Ta-rich partially ordered manganotantalite (i.e., some Mn and Fe occupying the B site, besides the A site, and some Ta and Nb occupying the A site, besides the B site), with orthorhombic structure. Heating in vacuum induces cation ordering (i.e., almost all Mn and Fe occupying the A site and Ta and Nb occupying the B site), but heating a powdered sample in air transforms it into wodginite, $\text{MnFeTa}_2\text{O}_8$, a monoclinic compound. Minor reflections on the XRPD pattern were indexed to $(\text{Fe}, \text{Mn})(\text{Ta}, \text{Nb})\text{O}_4$ with the ixiolite structure and to $(\text{Ta}, \text{Nb})_2\text{O}_5$. Another kind of transformation takes place when a crystal fragment is heated in air: a mixture of wodginite and almost ordered manganotantalite is observed, in addition to minor contributions from $(\text{Fe}, \text{Mn})(\text{Ta}, \text{Nb})\text{O}_4$ and $(\text{Ta}, \text{Nb})_2\text{O}_5$. The synthetic sample, $\text{Fe}(\text{Nb}, \text{Ta})_2\text{O}_6$, is a highly ordered ferrocolumbite, an orthorhombic compound. Heating in air transforms it to ixiolite, $\text{Fe}(\text{Nb}, \text{Ta})\text{O}_4$, with minor amounts of $(\text{Nb}, \text{Ta})_2\text{O}_5$.

Now we wish to discuss the consistence of the measured hyperfine parameters, when the crystallographic structures are concerned, and within the following constraints:

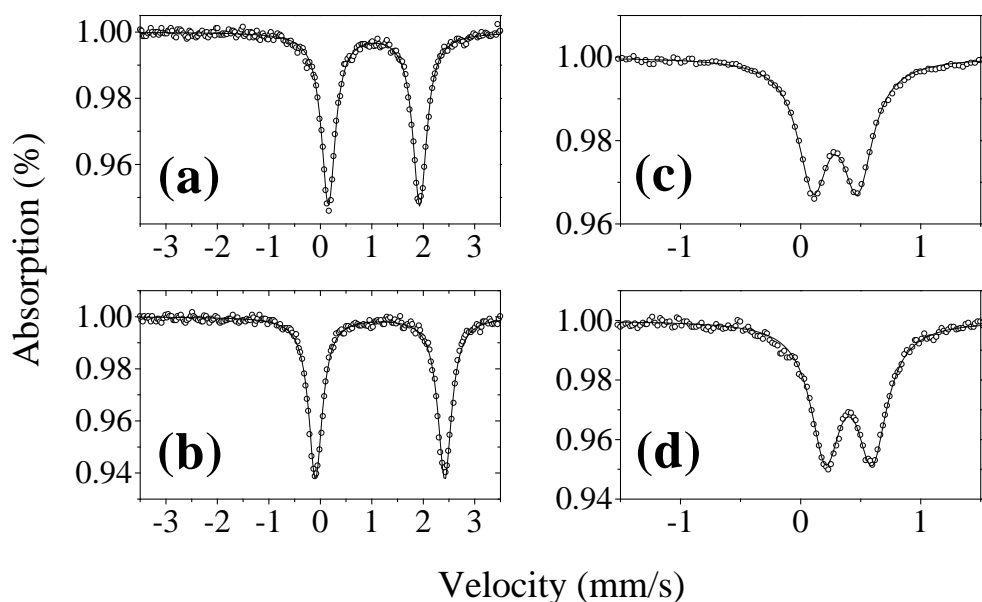


Figure 6. Mössbauer spectra for: (a) as-prepared $\text{Fe}(\text{Nb}_{0.6}\text{Ta}_{0.4})_2\text{O}_6$ sample taken at 300 K; (b) ditto, taken at 80 K; (c) powdered synthetic sample heated (PSH) in air taken at 300 K; (d) ditto, taken at 80 K. Open circles represent observed data. The solid lines represent the calculated spectra based on a least-squares procedure.

- (1) As the references used here are synthetic samples reported by other authors and all of them are ordered, only the natural sample heated in vacuum and our synthetic sample will be considered.
- (2) As the temperature dependence of the hyperfine parameters for all the samples are as expected, it is enough to discuss the room-temperature measurements. However, a brief comment should be presented concerning the LN spectrum for the PNH air sample. As can be seen in table 2, the relative area of the doublet assigned to FeO_6 octahedra is quite small as compared to that measured at RT. This may be due to a difference in the recoil free fractions on the two sites, but we have not data supporting this hypothesis. Therefore, although we are convinced on the experimental correctness of these results, we have not a clear explanation for them.
- (3) As far as the crystallographic structure is concerned, we need to consider only the quadrupole splitting parameter. It is not necessary to discuss the chemical aspect, what means that, here, the isomer shift plays a secondary role. However, it is important to note that all the isomer shifts reported here are consistent with those previously reported [9, 10, 14, 20–24].

For $(\text{Mn}_{0.88}\text{Fe}_{0.09})(\text{Ta}_{0.86}\text{Nb}_{0.14})_2\text{O}_6$, i.e. $(\text{Mn}, \text{Fe})\text{Ta}_2\text{O}_6$, we have observed two quadrupole doublets, both attributed to Fe^{2+} in octahedral coordination. As the AB_2O_6 structure presents only one crystallographic site for iron atoms, one of the observed doublets must be due to cation disorder. In fact, heat treatment in vacuum has induced cation ordering in this sample [9]. Accordingly the MS spectrum for the in-vacuum heat-treated sample showed just one quadrupole doublet, with $\Delta E_Q = 1.58 \text{ mm s}^{-1}$. For this reason we have attributed the smaller doublet to Fe^{2+} in FeO_6 octahedra and the larger one to Fe^{2+} in TaO_6 octahedra. The quadrupole splitting for FeO_6 ($\Delta E_Q = 1.58 \text{ mm s}^{-1}$) is smaller than that reported for FeNb_2O_6

($\Delta E_Q = 1.70 \text{ mm s}^{-1}$) [20]. These distinct values for ΔE_Q must be due to distinct Mn/Fe and Ta/Nb ratio concentrations.

This hypothesis can be analysed by considering the results from the synthetic $\text{Fe}(\text{Nb}_{0.6}\text{Ta}_{0.4})_2\text{O}_6$, for which we have measured $\Delta E_Q = 1.78 \text{ mm s}^{-1}$. Therefore, by comparing the measured ΔE_Q for FeNb_2O_6 and $\text{Fe}(\text{Nb}, \text{Ta})_2\text{O}_6$ it is reasonable to ascribe a small effect to the homopolar substitution $\text{Ta} \leftrightarrow \text{Nb}$. As shown above, the situation is quite different when FeNb_2O_6 and $(\text{Mn}, \text{Fe})\text{Ta}_2\text{O}_6$ are compared. In this case the measurements indicate that the homopolar substitution $\text{Mn} \leftrightarrow \text{Fe}$ is more effective in changing the hyperfine parameters than the $\text{Ta} \leftrightarrow \text{Nb}$ one. Considering the interdependence between quadrupole splitting and distortions of the metal–oxygen octahedra, and taking into account the ionic radii, these results seem to be consistent, since $R_{\text{Mn}^{2+}}/R_{\text{Fe}^{2+}} \cong 1.08$, while $R_{\text{Nb}^{5+}}/R_{\text{Ta}^{5+}} \cong 1.01$. Therefore the effect of the homopolar substitution $\text{Mn} \leftrightarrow \text{Fe}$ on the distortions of the metal–oxygen octahedra (MO_6) is stronger than that produced by the $\text{Ta} \leftrightarrow \text{Nb}$ one. This is consistent with structure refinement performed on similar samples [10], which have shown that the unit-cell volume is mainly a function of the $\text{Mn} \leftrightarrow \text{Fe}$ substitution, while $\text{Ta} \leftrightarrow \text{Nb}$ substitution has only a minor influence on the cell volume. The authors of [10] have also shown that FeO_6 octahedra are more distorted than the TaO_6 ones, supporting the site assignment given above. As it is known [25], Fe^{2+} high spin compounds in which the crystal field contribution to the electric field gradient is relevant show a decreasing of the quadrupole splitting as the octahedral distortion increases.

For ixiolite $\text{Fe}(\text{Nb}, \text{Ta})\text{O}_4$ (PSH air) we have observed a single doublet with $\Delta E_Q = 0.37 \text{ mm s}^{-1}$. To the best of our knowledge this is the first report on the hyperfine parameters for Nb-rich samples of the $\text{Fe}(\text{Nb}, \text{Ta})\text{O}_4$ type. However it is possible to appreciate the consistency of our measurement, taking into account that reported for FeTaO_4 , with the rutile structure, i.e., $\Delta E_Q = 0.53 \text{ mm s}^{-1}$ [22]. As discussed above, the homopolar substitution $\text{Ta} \leftrightarrow \text{Nb}$ presents a minor effect on the hyperfine parameters of these compounds. The reported results strongly suggest that the hyperfine parameters are more dependent on the crystal structure. Thus, if for columbite $\Delta E_Q \cong 1.70 \text{ mm s}^{-1}$ [20, 21], and for tapiolite $\Delta E_Q \cong 3.0 \text{ mm s}^{-1}$ [23, 24], it appears reasonable that ΔE_Q for ixiolite $\text{Fe}(\text{Nb}, \text{Ta})\text{O}_4$ should be smaller than for rutile FeTaO_4 . This becomes consistent if we take into account the interrelation between crystal structures. That is to say, the substructures (ixiolite and rutile) preserve the interrelation observed between the superstructures (columbite and tapiolite).

In addition to the consistency shown by the analysis above, it is interesting to point out that the present results confirm the data of Moreau and Tramasure [26]. These authors have synthesized a wodginite from the reaction $\text{Mn}_2\text{O}_3 + \text{Ta}_2\text{O}_5$ at 1040°C for 95 h in air, suggesting that Mn plays an important role in the tantalite \rightarrow wodginite transformation. We have also reproduced early results reported by Gouder de Beauregard *et al* [13], demonstrating that upon heating in air $(\text{Mn}, \text{Fe})\text{Ta}_2\text{O}_6$ shows an XRPD pattern quite similar to that of $\text{MnFeTa}_2\text{O}_8$.

6. Conclusions

Heating in air a disordered $(\text{Mn}_{0.88}\text{Fe}_{0.09})(\text{Ta}_{0.86}\text{Nb}_{0.14})_2\text{O}_6$ sample yields different result depending on the form of the sample. For a powder sample, the $(\text{Mn}_{0.88}\text{Fe}_{0.09})(\text{Ta}_{0.86}\text{Nb}_{0.14})_2\text{O}_6 \rightarrow \text{MnFeTa}_2\text{O}_8$ transformation has been observed, in addition to a minor contribution from $(\text{Mn}, \text{Fe})(\text{Ta}, \text{Nb})\text{O}_4$ and $(\text{Ta}, \text{Nb})_2\text{O}_5$. For a crystal fragment, the heat treatment in air produced a mixture of four phases: that in largest amount is the ordered $(\text{Mn}_{0.88}\text{Fe}_{0.09})(\text{Ta}_{0.86}\text{Nb}_{0.14})_2\text{O}_6$, while minor contributions are attributed to $\text{MnFeTa}_2\text{O}_8$, $(\text{Mn}, \text{Fe})(\text{Ta}, \text{Nb})\text{O}_4$ and $(\text{Ta}, \text{Nb})_2\text{O}_5$. The former arrives from cation ordering in the bulk portion of the sample, while the minor contributions result from the near-surface

oxidation. The Mn content as well as the oxidant atmosphere appears to play an important role in the tantalite–wodginite transformation. The same heat treatment applied to a powder synthetic ferrocolumbite, $Fe(Nb_{0.6}Ta_{0.4})_2O_6$, induces a different reaction: the sample is transformed into $Fe(Nb_{0.6}Ta_{0.4})O_4$ with a minor amount of $(Nb, Ta)_2O_5$.

The hyperfine parameters measured for the heat-induced wodginite are quite similar to those previously reported [14]. The heat-induced $Fe(Nb_{0.6}Ta_{0.4})O_4$ sample presents an x-ray diffraction pattern and Mössbauer parameters consistent with an ixiolite-like crystallographic structure.

Acknowledgments

We would like to thank Drs M Adusumilli (UNB, Brazil) and J-Y Henri (DRFMC/CENG, Grenoble) for providing us with the natural manganotantalite and the synthetic ferrocolumbite, respectively, used in this work. We are indebted to Dr P M Mors and Professor L Amaral for a critical reading of the manuscript. Valuable discussions with Professor F C Zawislak are gratefully acknowledged. This work was supported in part by the Brazilian agencies CAPES, CNPq, FAPERGS and FINEP.

References

- [1] Cerný P and Ercit T S 1985 *Bull. Minéral.* **108** 499
- [2] Graham J and Thornber M R 1974 *Am. Mineral.* **59** 1026
- [3] Nickel E H, Rowland J F and McAdam R C 1963 *Can. Mineral.* **7** 390
- [4] Nickel E H, Rowland J F and McAdam R C 1963 *Am. Mineral.* **48** 961
- [5] Ferguson R B, Hawthorne F C and Grice J D 1976 *Can. Mineral.* **14** 550
- [6] Cerný P, Ercit T S and Wise M A 1992 *Can. Mineral.* **30** 587
- [7] Grice J D, Ferguson R B and Hawthorne F C 1976 *Can. Mineral.* **14** 540
- [8] Ercit T S, Hawthorne F C and Cerný P 1992 *Can. Mineral.* **30** 597
- [9] Zawislak L I, Antoniotti V, da Cunha J B M and dos Santos C A 1997 *Solid State Commun.* **101** 767
- [10] Wenger M, Armbruster T and Geiger C A 1991 *Am. Mineral.* **76** 1897
- [11] Ercit T S, Wise M A and Cerný P 1995 *Am. Mineral.* **80** 613
- [12] Turnock A C 1966 *Can. Mineral.* **8** 461
- [13] Gouder de Beauregard C G, Dubois J and Bourguignon P 1967 *Ann. Soc. Géol. Belgique* **90** 501
- [14] Ercit T S, Cerný P, Hawthorne F C and McCammon C A 1992 *Can. Mineral.* **30** 613
- [15] Adusumilli M S 1976 Contribution to the Mineralogy of Niobotantalites from the Northeast Province *PhD Thesis* Universidade Federal de Minas Gerais, Brazil (in Portuguese)
- [16] Rodriguez-Carvajal J 1997 Short reference guide of the program FullProf, version 3.2, available in 'pub/divers/fullp' of the anonymous ftp area of the LLB unix cluster
- [17] Long G J, Cranshaw T E and Longworth G 1983 *Mössbauer Eff. Ref. Data J.* **6** 42
- [18] Bourguignon P and Mélon J 1965 *Ann. Soc. Géol. Belgique* **88** 291
- [19] Roth R S and Waring J L 1964 *Am. Mineral.* **49** 242
- [20] Eibschütz M, Ganiel U and Shtrikman S 1967 *Phys. Rev.* **156** 259
- [21] Yaeger I, Morrish A H, Boumford C, Wong C P, Wanklyn B M and Garrard B J 1978 *Solid State Commun.* **28** 651
- [22] Astrov D N, Kryukova N A, Zorin R B, Makarov V A, Ozerov R P, Rozhdestrvenskii F A, Smirnov V P, Turchaninov A M and Fadeeva N V 1973 *Sov. Phys.-Crystallogr.* **17** 1017
- [23] Eicher S M, Greedan J E and Lushington K J 1986 *J. Solid. State Chem.* **62** 220
- [24] Zawislak L I, da Cunha J B M, Vasquez A and dos Santos C A 1995 *Solid State Commun.* **94** 345
- [25] Bancroft G M 1973 *Mössbauer Spectroscopy. An Introduction for Inorganic Chemists and Geochemists* (London: McGraw-Hill) p 252
- [26] Moreau J and Tramasure G 1965 *Ann. Soc. Géol. Belgique* **88** 301